Chapter 1

Introduction

One of the basic questions in physics is about the origin of the structure of matter. From the ancient times, a great number of philosophers and scientists have been trying to answer the questions that deal with the constituents of matter forming the ultimate structure of the universe. Although most of the early notions and predictions about the structure of matter were found out to be wrong, nevertheless they formed a basis for the theories developed centuries later with the improved knowledge of physicists. It is only at the present time of the 21st century, a more precise and consistent picture of the building blocks of matter has evolved that reaches from the atomic model up to the present elementary particles. Particle physics is the field of natural science which mainly deals with the fundamental constituents of matter and the interactions among them.

The theory that currently describes all the phenomena of particle physics in terms of the properties and interactions of the elementary particles, which also includes the results of experimental and theoretical investigations of many years is known as the Standard Model (SM) of particle physics. According to this theory, the fundamental constituents of matter are the two half-integer spin families of fermions called leptons and quarks. There are three generations of leptons and quarks and they interact via the exchange of gauge bosons. They are the integer-spin elementary particles mediating the fundamental interactions. Each type of these fundamental interactions corresponds to

some kind of the gauge boson: the photon γ act as a mediator for the electromagnetic interaction; the heavy gauge bosons, Z^0 and $W^{\pm}$, carry the weak interaction; and the eight gluons g mediate the strong interaction. Thus the main component of the SM [1,2] are the electroweak theory which unifies the electromagnetic and weak interactions and the strong interactions described by Quantum Chromodynamics (QCD) [3, 4]. In addition, a new spin-zero boson, named Higgs boson has been also included recently in the model. This Higgs boson is responsible for the acquisition of mass by elementary particles. Despite being the most successful theory in particle physics, SM is not completely perfect as there are still some fundamental questions which need to be further clarified. It does not explain one of the natural phenomena gravity, the nature of dark matter and dark energy, neutrino masses and matter-antimatter asymmetry etc.

The behaviour of quarks and gluons is mainly described by QCD, the theory of strong interaction. This theory describes interactions of quarks via the exchange of gluons. Due to the non-abelian nature of QCD [5, 6], the strength of the interaction between the quarks decreases towards small distance and they behave as free particles. This behaviour is called asymptotic freedom [4]. With the increase of distance, the strength of the interaction rises and the quarks cease to behave as free particles. Rather, they behave as composite particles which explains the confinement of quarks [7]. Both these interesting phenomena of QCD implies that gluons carry colour charge and indicate the self interaction property of gluons. Thus, it is important to study the processes involving gluons.

The proton is one of the familiar particles around us. As it consists of the fundamental particles, quarks and gluons, a detailed study of its internal structure is one of the fascinating topics in QCD. The knowledge of its structure is important for perturbative QCD (pQCD) calculations of any process involving proton. Its structure also helps to explain the origin of matter. In the present particle accelerators and colliders, scattering experiments are conducted to test the theoretical predictions of the SM

and also to have the opportunity to search for new physics concerning the basic laws governing the interactions between the elementary particles. The knowledge of proton structure and QCD is a vital tool which helps to interpret the potential signals of new physics at the Large Hadron Collider (LHC) at CERN.

The scattering experiments have played an important role in the elementary particle physics research starting from Rutherford's experiment [8], which explained the structure of atom in 1911 or later the Stanford Linear Accelerator Center (SLAC) experiments, which revealed the partonic structure of nucleon in 1969 [9, 10]. SLAC allowed to study the Deep Inelastic Scattering (DIS) processes for the first time i.e., scattering at high values of momentum transfer from electrons to protons. Among the scattering experiments, the electron-proton scattering is an important one. Being leptons, electrons are small in size and possess other well known properties of leptons. These properties help the electrons to penetrate deep inside the proton and thus they are able to test the proton structure very precisely.

The electron-proton collider, Hadron Elektron Ringanlage (HERA) located at the Deutsches Elektronen Synchrotron (DESY) in Hamburg, Germany operated from year 1992 to 2007. HERA gave a unique opportunity to investigate the structure of proton over a wide kinematic range of Bjorken variable x (down to 10^{-6}) and squared four momentum transferred between lepton and proton Q^2 (up to 10^6 GeV^2) where the dynamics of DIS become dominated by gluon. It collected e^+p collision data with the H1 and ZEUS detectors at a positron beam energy of 27.5 GeV and a proton beam energies of 920, 575 and 460 GeV, which allowed a measurement of structure functions at x values $2.9 \times 10^{-5} \leq x \leq 0.01$ and Q^2 values $1.5GeV^2 \leq Q^2 \leq 800GeV^2$ [11, 12]. HERA also collected data for inclusive charm and beauty cross sections and the derived heavy flavour structure function in e^-p and e^+p neutral current collisions in the kinematical range of x values $2 \times 10^{-4} \leq x \leq 0.05$ and Q^2 values $5GeV^2 \leq Q^2 \leq 2000GeV^2$ [13].

At low values of x, the proton structure is analysed by gluon dominance. In

pQCD the gluon distribution is determined indirectly by Q^2 dependence of DIS cross section. This determination is directly affected by pQCD calculations. The proton structure is basically described in terms of structure functions, F_2, xF_3 and F_L. Among them F_L is directly related to gluon density in the proton. As its sensitivity towards gluon density is somewhat different from the scaling violation, F_L is expected to give a test of pQCD validity. Theoretically, the measurement of F_L structure function helps us to distinguish different models describing the QCD evolution at small-x. In fact, the structure function measurement remains incomplete until the measurement of longitudinal structure function is actually included in the study.

Heavy quark production at HERA is of particular interest for testing various calculations in pQCD. The heavy quark masses, as well as the transverse momentum of a jet, provide a hard scale, which is essential for the calculations in pQCD predictions [14]. As it is well known, that the scaling violations are different in the massless and massive pQCD cases, therefore, in all precision measurement, along with the light flavour, a detailed treatment of heavy flavour contribution is also required. The measurements of heavy quark uniquely constrain the parton distribution functions (PDFs) of proton, mainly its charm (c) and beauty (b) contents. The precise knowledge of PDFs is also essential at LHC. The b quark density plays an important role in Higgs production at the LHC along with the extensions to the standard model such as supersymmetric models at high values of the mixing parameter tanβ [15]. The dominant process for the charm and beauty quark production at HERA is the Boson Gluon Fusion (BGF), where the photon interacts with a gluon from the proton by the exchange of a heavy quark pair and is given as $\gamma g \rightarrow q\bar{q}X$, with $q = c, b$ [16]. This indicates that the process is sensitive to the gluon density in the proton.

In this thesis work, we have mainly studied the small-x behaviour of proton longitudinal structure function F_L. The thesis is organised as follows: in the next sections of this chapter the overview of DIS, proton structure functions and their experimental mea-

surement, quark parton model, quantum chromodynamics, QCD evolution equations, longitudinal structure function F_L, DIS experiments related to F_L structure function, small-x physics, heavy quark contribution to structure functions are given. The 2nd chapter describes the behaviour of F_L structure function from QCD evolution equation using Taylor series expansion method. In 3rd chapter, the behaviour of F_L structure function from QCD evolution equation is analysed using Regge behaviour of structure function and comparison between the results obtained in both the methods is studied. In 4th chapter, we have studied the approximate relation between F_L and gluon distribution function using Taylor expansion method and studied the evolution of F_L structure function with respect to x. In 5th chapter, the behaviour of structure function F_L is studied using the gluon distribution function obtained as a solution of the DGLAP evolution equation and comparative study of the results with the results of 4th chapter is presented. 6th chapter describes the contribution of heavy quark to F_L structure function using Taylor expansion method and Regge behaviour of gluon distribution function and the comparative analysis of the results obtained by both the methods. In chapter 7, we summarise the overall conclusion and future directions of our study.

1.1 Deep Inelastic Scattering

Deep Inelastic Scattering (DIS) is the basic tool for understanding the inside structure of nucleon and the interaction dynamics of quarks and gluons. Since the discovery of structure of proton at SLAC fixed target experiment in 1969 [9], these measurement have played an important role in the development of the theory of strong interactions, Quantum Chromodynamics. DIS is the process in which constituents of proton are probed by means of lepton-proton scattering. The process is 'inelastic' as when a quark knocks out of the proton, the proton is broken up, producing a jets of hadron. It is

called 'deep', here the proton is probed with a high energetic gauge boson i.e., with small wavelength to resolve its structure up to small distance scale. In this process when the exchange boson is a neutral particle, photon γ or a neutral vector boson Z^0, it is referred to as neutral current DIS and if the exchange particle is a charged boson, $W^{\pm}$, it is known as charged current DIS. Figure 1.1 defines the kinematics of DIS process in terms of following four-vectors, k: initial state lepton; k': final state lepton; P: final state proton and $q = k - k'$: the exchange field quantum. A measurement summing up all the final states in the hadronic system is known as inclusive measurement. The inclusive DIS process can be described in terms of the following kinematic variables:

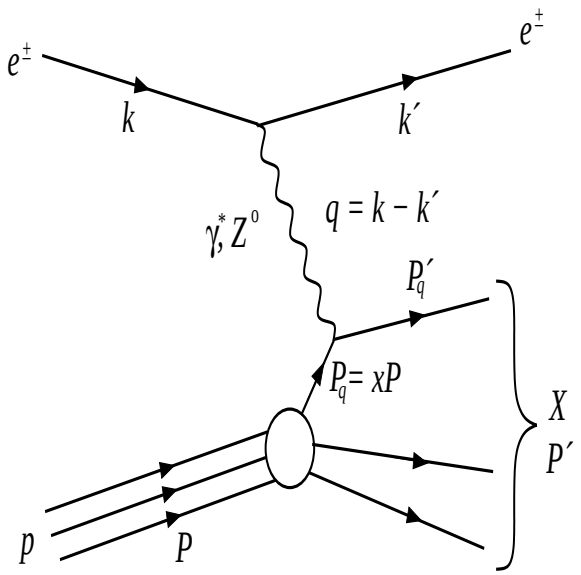

Figure 1.1: Feynmann diagram of Deep Inelastic Scattering

- The negative of the four-momentum transferred to the photon which qualitatively determines the scale of the interaction

$$Q^2 = -q^2 = -(k - k')^2 \tag{1.1}$$

- The fraction of proton momentum carried by the struck quark known as Bjorken

scaling variable

$$x = \frac{Q^2}{2P \cdot q} \tag{1.2}$$

- The inelasticity variable which corresponds to the fraction of the incoming lepton energy transfer by the exchanged boson to the proton in the proton rest frame

$$y = \frac{P \cdot q}{P \cdot k} \tag{1.3}$$

- Center of mass energy squared

$$s = (k + P)^2 \tag{1.4}$$

- The invariant mass squared W^2 of the produced hadronic final state

$$W^2 = (q + P)^2 \tag{1.5}$$

The variables Q^2, x, y and s defined above are related by the equation

$$Q^2 = (s - M_P^2)xy, \tag{1.6}$$

where M_P^2 is the mass of the proton. This relation (1.6) implies that at a given ep center of mass energy $\sqrt{s}$, any two of the variables Q^2, x, y are enough to describe the kinematics of DIS process, usually Q^2 and x are used. Here both the dimensionless variables x and y are limited to values between 0 and 1. The values of Q^2 and W^2 lies between 0 and s, M_P and $\sqrt{s}$ respectively [17].

The invariant mass squared W^2 of final hadronic state can also be written in terms of Q^2 and x as [18]

$$W^2 = M_P^2 + Q^2\Big(\frac{1-x}{x}\Big). \tag{1.7}$$

This equation (1.7) explains that at fixed Q^2, low-x interaction corresponds to large values of the invariant mass squared W^2 of final hadronic state. It also signifies the term 'deep' and 'inelastic' corresponds to $Q^2 \gg M_P^2$ and $W^2 \gg M_P^2$ respectively. Thus, the value of the proton mass M_P may be neglected in the last two equations.

1.2 DIS Cross Section and Structure Functions

In inclusive DIS experiment, one of the important quantity to measure is the scattering cross section. The cross section of the lepton-proton scattering can be written in terms of leptonic and hadronic part as [19]

$$d\sigma \sim L_{\mu\nu} W^{\mu\nu}, \tag{1.8}$$

where $L_{\mu\nu}$ denotes the leptonic tensor describing the interaction between the lepton and the virtual exchanged gauge boson and $W^{\mu\nu}$ represents the hadronic tensor which corresponds to the boson-proton interaction. Neglecting the electron mass, the leptonic tensor which is well known in Quantum Electrodynamics (QED) can be written as [20]

$$L_{\mu\nu} = 2(k'_{\mu} k_{\nu} + k'_{\nu} k_{\mu} - (k' \cdot k) g_{\mu\nu}), \tag{1.9}$$

where $g_{\mu\nu}$ denotes the metric tensor. The hadronic tensor describing the hadron vertex has the form [17]

$$\begin{aligned} W^{\mu\nu} &= -W_1 g^{\mu\nu} + \frac{W_2}{M_P^2} p^{\mu} p^{\nu} - i\varepsilon^{\mu\nu\alpha\beta} p_{\alpha} q_{\beta} \frac{W_3}{2M_P^2} + q^{\mu} q^{\nu} \frac{W_4}{M_P^2} \\ &\quad + (p^{\mu} q^{\nu} + q^{\mu} p^{\nu}) \frac{W_5}{M_P^2} + i(p^{\mu} q^{\nu} - p^{\nu} q^{\mu}) \frac{W_6}{2M_P^2}, \end{aligned} \tag{1.10}$$

where M_P is the mass of proton, W_i are Lorentz scalar function of x and Q^2 which describes the structure of proton. If the scattering process involves only γ exchange, the parity violating term W_3 and also antisymmetric term W_6 are absent. The current conservation at the hadronic vertex gives $q_{\mu} W^{\mu\nu} = q_{\nu} W^{\mu\nu} = 0$ so that

$$W_5 = -\frac{p \cdot q}{q^2} W_2, \tag{1.11}$$

$$W_4 = \Big(\frac{p \cdot q}{q^2}\Big)^2 W_2 + \frac{M_P^2}{q^2} W_1. \tag{1.12}$$

Thus, the hadronic tensor depends on W_1 and W_2 only and can be written as

$$W^{\mu\nu} = W_1\Big(- g^{\mu\nu} + \frac{q^{\mu} \cdot q^{\nu}}{q^2}\Big) + \frac{W_2}{M_P^2}\Big(p^{\mu} - \frac{p \cdot q}{q^2} q^{\mu}\Big)\Big(p^{\nu} - \frac{p \cdot q}{q^2} q^{\nu}\Big). \tag{1.13}$$

The functions W_1 and W_2 are redefined in terms of structure functions of proton F_1 and F_2 as

$$F_1(x, Q^2) = M_P W_1(x, Q^2), \tag{1.14}$$

$$F_2(x, Q^2) = \frac{p \cdot q}{M_P} W_2(x, Q^2). \tag{1.15}$$

Thus, the double differential DIS cross section can be expressed using structure function $F_1(x, Q^2)$ and $F_2(x, Q^2)$ in the form

$$\frac{d^2\sigma}{dxdQ^2} = \frac{4\pi\alpha^2}{xQ^4}\Big[\frac{y^2}{2} 2xF_1(x, Q^2) + (1-y)F_2(x, Q^2)\Big], \tag{1.16}$$

here α is the fine structure constant. The structure functions $F_1(x, Q^2)$ is proportional to the transverse component of the cross section and the difference between $F_2(x, Q^2)$ and $F_1(x, Q^2)$ gives the longitudinal part of the cross section. Thus, the longitudinal structure function is defined as

$$F_L(x, Q^2) = F_2(x, Q^2) - 2xF_1(x, Q^2). \tag{1.17}$$

Now, the cross section in terms of $F_2(x, Q^2)$ and $F_L(x, Q^2)$ structure functions can be written as

$$\frac{d^2\sigma}{dxdQ^2} = \frac{2\pi\alpha^2 Y_+}{xQ^4}\Big[F_2(x, Q^2) - \frac{y^2}{Y_+} F_L(x, Q^2)\Big], \tag{1.18}$$

where $Y_+ = 1 + (1-y)^2$ is a function of y. Since the contribution of F_L structure function to DIS cross section is proportional to the factor $\frac{y^2}{Y_+}$, the F_2 term dominates at $y < 0.5$ and the contribution of F_L structure function is significant towards the total cross section at large values of $y \geq 0.5$ [21]. In DIS experiment structure functions are extracted from the measured cross section. Therefore, it is convenient to define the reduced cross section as

$$\sigma_r = F_2(x, Q^2) - \frac{y^2}{Y_+} F_L(x, Q^2). \tag{1.19}$$

The ep scattering process can also be considered as the interaction of a flux of virtual photon and the proton. In terms of the two components of the cross section i.e., transverse and longitudinal cross section, the double differential cross section can be written as

$$\frac{d^2\sigma}{dxdQ^2} = \Gamma(y)[\sigma_T(x,Q^2) - \epsilon(y)\sigma_L(x,Q^2)]. \tag{1.20}$$

Here σ_T and σ_L corresponds to the absorption cross section for transversely and longitudinally polarised virtual photon respectively, $\Gamma(y) = \frac{\alpha^2 Y_+}{2\pi x Q^2(1-x)}$ stands for the photon flux and $\epsilon(y) = \frac{2(1-y)}{Y_+}$ defines the virtual photon polarisation.

Now, comparing the equations (1.18) and (1.20) one can express the above mentioned structure function in terms of the virtual photon absorption cross section as

$$F_2(x,Q^2) = \frac{Q^2(1-x)}{4\pi^2\alpha}[\sigma_T(x,Q^2) + \sigma_L(x,Q^2)], \tag{1.21}$$

$$F_L(x,Q^2) = \frac{Q^2(1-x)}{4\pi^2\alpha}\sigma_L(x,Q^2). \tag{1.22}$$

Equation (1.22) indicates that the longitudinal structure function is directly proportional to the longitudinal component of the cross section. From the equations (1.21) and (1.22), as the measured quantity σ cannot be negative, the two structure functions $F_2(x,Q^2)$ and $F_L(x,Q^2)$ obey the relation

$$0 \leq F_L(x,Q^2) \leq F_2(x,Q^2). \tag{1.23}$$

Another quantity which represents the relation between the cross sections of the absorption of a longitudinal and transverse polarized photon by hadron is the ratio $R(x,Q^2)$ and is given by

$$R(x,Q^2) = \frac{\sigma_L}{\sigma_T} = \frac{F_L(x,Q^2)}{F_2(x,Q^2) - F_L(x,Q^2)}. \tag{1.24}$$

At small values of x, this ratio $R(x, Q^2)$ gives the relative strength of the two components of the cross section [22]. $R(x, Q^2)$ provides the information about the spin and transverse momentum of the constituents of the nucleon [23] which is explained in the next section.

1.3 Quark Parton Model

The Quark Parton Model (QPM), introduced by Feynman, explains that the proton is made up of point like constituents known as partons [24]. The basic idea of the parton model was based on the experimental observation of Bjorken scaling [25], that is in the ep scattering experiment at SLAC it was observed that the structure function measured at fixed values of x are approximately independent of the four-momentum transfer Q^2 from the probe to the nucleon and depend only on the variable x [9, 10]. This behaviour was predicted by Bjorken and suggested that the proton is consists of point-like particle, called as parton. According to this model, the proton consists of quasi-free point-like particles which were identified as quarks, particle with spin-$\frac{1}{2}$ and electric charge $\pm\frac{1}{3}e$ or $\pm\frac{2}{3}e$, as proposed by Gell-Mann [26] and Zweig [27]. The proton consists of two u quarks with charge $+\frac{2}{3}e$ and one d quark with charge $-\frac{1}{3}e$.

In the QPM, the deep inelastic ep scattering is interpreted as the elastic scattering between the lepton and quarks. The ep cross section is then incoherent sum over all lepton-quark scattering cross section. Here incoherent means that the lepton scatters on a single quasi-free quark. With these assumptions, the structure functions F_1 and F_2 can be expressed as a sum of quark momentum distributions $xq(x)$ weighted with the square of their electric charge e_i:

$$F_1(x, Q^2) = \frac{1}{2x} \sum_i e_i^2 x q_i(x), \tag{1.25}$$

$$F_2(x, Q^2) = \sum_i e_i^2 x q_i(x), \tag{1.26}$$

here e_i is the charge of the parton i and $q_i(x)$ is the probability that the quark i carries a fraction of proton momentum in the interval $[x, x + dx]$. The sum runs over all the partons in the proton. Hence, in QPM the structure functions F_1 and F_2 depend only on the variable x as predicted by Bjorken.

The cross sections σ_T and σ_L depend on the spins of the proton constituents. As the longitudinal virtual photon cannot interact with the spin-$\frac{1}{2}$ quarks due to helicity conservation [28] at the hadronic vertex, the model predicts $\sigma_L = 0$ which leads to

$$F_L(x, Q^2) = F_2(x, Q^2) - 2xF_1(x, Q^2) = 0 \tag{1.27}$$

and consequently gives

$$F_2(x, Q^2) = 2xF_1(x, Q^2), \tag{1.28}$$

which is known as the Callan Gross relation [28] and reflects the spin-$\frac{1}{2}$ nature of the quarks. The cross section ratio R, mentioned in the section 1.2 is often used instead of F_L to describe the scattering cross section. In the framework of QPM with spin-$\frac{1}{2}$ quark, R is expected to be small, and to decrease rapidly with increasing momentum transfer Q^2. Measurement of R at SLAC also indicated that the scattering from the spin-$\frac{1}{2}$ constituents of the nucleon (quarks) dominates [29–31].

The QPM cannot explain all the properties of DIS. Since the naive QPM predicts that the proton is made up of two up (u) and one down (d) valance quarks, the total momentum of the quarks inside the proton should be 1. But the experimental results [30] show that quarks carry only half of the proton's momentum, i.e.

$$\int_0^1 [xu(x) + xd(x)]dx = 0.54. \tag{1.29}$$

This clearly suggests that there is more momentum in proton than that carried by quarks. This fact provided the first indirect evidence of the gluonic component of the proton. Another drawback is the observation of scaling violation of F_2 measured in different experiments. The scaling behaviour is observed only for values of about $x < 0.1$ and brakes for $x > 0.1$. Structure function measurement at H1 experiment [32] and some other fixed target experiment [33] shows the dependency of F_2 on Q^2. To explain the mentioned discrepancies the theory of quantum chromodynamics plays an important role, which is described in the next section.

1.4 Quantum Chromodynamics

Quantum Chromodynamics (QCD) is the theory which describe the strong interaction between the quarks and gluons inside the proton [5, 6]. The key point in this theory is that the quarks and gluons have a quantum number called colour, which is described by $SU(3)$ symmetry group and can be represented by three colours - red, green and blue. The quarks can interact by the exchange of a massless and electrically neutral spin-1 boson called gluons. QCD is a non-abelian $SU(3)$ gauge theory [6]. As a result, there are eight gluons and they also interact among themselves via the exchange of colour charge. Hadrons are considered to be colourless or colour singlets of the group $SU(3)$ constructed from the fundamental colour triplet of quarks. Only colourless particles can exist as free particles. Thus the quarks and gluons cannot be observed as free one rather they should always be confined within the hadron. This property of QCD is known as confinement. An important feature of quantum field theories is the running coupling constant, i.e., the coupling evolves with the energy scale of the interaction. Because of the non-abelian nature of gauge group $SU(3)$, opposite to $U(1)$ group of QED, the strong coupling constant α_s shows the opposite behaviour with that of the electromagnetic fine structure constant α. This leads to asymptotic freedom

which predicts that at large energy scales Q^2 the coupling between quarks and gluons decreases and they behave as free particles, while at lower energies they were confined to colourless hadron.

The strong coupling constant α_s is one of the important characteristics of strong interaction. The lowest order i.e., Leading Order (LO) of α_s does not include any gluon vertices. In Next-to-Leading Order (NLO), the interaction between quarks and gluons are included and more gluon vertices are added in higher orders. In LO approximation the coupling constant α_s is given by the equation [34]

$$\alpha_s(Q^2) = \frac{12\pi}{(33 - 2N_f)\ln\frac{Q^2}{\Lambda^2_{QCD}}}, \tag{1.30}$$

where N_f is the number of active quark flavours. Λ_{QCD} characterizes the strength of the coupling and is the order of $300 - 500MeV$. The phenomenon of confinement is described at $Q^2 < \Lambda^2_{QCD}$. Contrary to it, for large energy scales $Q^2 > 1GeV^2$, perturbative calculations are possible in QCD using order-by-order expansion in α_s [35].

According to QCD, protons not only consists of quarks but also gluons which binds the quarks inside the proton. Due to the presence of gluons, some modifications take place in the quark parton model as the quarks can interact via the exchange of gluons and can also radiate gluons. The radiated gluons can split into quark-antiquark pairs or gluons. Thus a quark seen at an energy scale Q_0^2 carrying a momentum fraction x_0 can be resolved into more quarks and gluons at a higher values of Q^2, i.e., $Q_1^2 > Q_0^2$ and lower values of $x_1 < x_0$. As a result the structure function shows Q^2 dependence violating the Bjorken scaling.

The pQCD calculations in DIS process can be expressed using factorization theorem [36]. This theorem provides a systematic way to refine the predictions of the parton model. In this theorem, the cross section involving hadron can be expressed as two distinct part: one short distance and the other long distance parts [37]. The short

distance or hard process part which is process dependent can be calculated perturbatively using renormalizable theory of QCD. On the other hand, the long distance part which is process independent and unpredictable requires experimental results. This part involves the PDFs into which infrared divergences of QCD are absorbed. Factorization theorem leads to the expression for F_2 structure function as the convolution of co-efficient function C_2^i and the parton distribution function f_i [38] :

$$F_2(x,Q^2) = \sum_{i=q,g} \int_x^1 dw C_2^i\Big(\frac{x}{w}, \frac{Q^2}{\mu_r^2}, \frac{\mu_f^2}{\mu_r^2}, \alpha_s(\mu_r^2)\Big) f_i(w,\mu_r^2,\mu_f^2). \tag{1.31}$$

Here the co-efficient function C_2^i represents the hard scattering matrix element for the interaction of the photon with a parton i which can be calculated using perturbative expansion in α_s. The parton distribution function f_i is the probability to find a parton i carrying a fraction w of the proton's momentum. In this process the summation is over all the partons. The factorization scale μ_f defines the boundary between the long distance and short distance part. The renormalization scale μ_r defines the separation between the finite and divergent contributions in the renormalization procedure. Both the scales μ_r and μ_f are arbitrary and helps to absorb the infrared and ultraviolet divergences in pQCD. There are several renormalization schemes used in the calculations of QCD. Among them the most commonly used one is the modified minimal subtraction ($\overline{MS}$) scheme [38]. Here, renormalized quark distribution absorbs the divergent part of the co-efficient functions at $\mu_r = \mu_f$. And another useful scheme is DIS scheme where one chooses $\mu_r = \mu_f = Q$. Therefore one can write the expression for F_2 as

$$F_2(x,Q^2) = \sum_i e_i^2 x f_i(x,Q^2), \tag{1.32}$$

which reflects the Q^2 dependence of the structure function. Also F_L gives non-zero value and this can be obtained from F_2 and the gluon density $G(x,Q^2)$ which is explained in the section 1.5. Since F_L is directly related to cross section ratio R, thus R is also non

zero. In QCD, the value of R is proportional to the QCD coupling constant α_s [23].

QCD Evolution Equations:

An important outcome of the factorization theorem is that the measurement of parton distribution function at one scale Q_0 allows one to calculate it for any other scale Q'. This property of parton distribution is known as evolution. The evolution equations can describe the behaviour of quark $q_i(x, Q^2)$ and gluon $g(x, Q^2)$ distribution function with the scale of interaction Q^2.

The parton distribution in the hadron cannot be calculated from the first principles, involving the building blocks of hadronic matter, the quarks and gluons, and their mutual interactions as described by QCD. With the help of the factorization theorem, the parton evolution, the Q^2 dependence of partons can be calculated within pQCD. These evolution equations of parton are known as Dokshitzer-Gribov-Lipatov-Altarelli-Parisi (DGLAP) evolution equations [35,39–41]. These describe the evolutions of quark $q_i(x, Q^2)$ and gluon $g(x, Q^2)$ distribution function with the scale of interaction Q^2 :

$$\frac{dq_i(x,Q^2)}{dlnQ^2} = \frac{\alpha_s(Q^2)}{2\pi}\int_x^1 \frac{dw}{w}\left[\sum_j q_j(w,Q^2)P_{ij}\Big(\frac{x}{w}\Big) + g(w,Q^2)P_{ig}\Big(\frac{x}{w}\Big)\right], \tag{1.33}$$

$$\frac{dg(x,Q^2)}{dlnQ^2} = \frac{\alpha_s(Q^2)}{2\pi}\int_x^1 \frac{dw}{w}\left[\sum_j q_j(w,Q^2)P_{gj}\Big(\frac{x}{w}\Big) + g(w,Q^2)P_{gg}\Big(\frac{x}{w}\Big)\right]. \tag{1.34}$$

Here, the function $P_{ij}\Big(\frac{x}{w}\Big)$ is known as the splitting functions which describes the probability that a parton i with momentum fraction x is emitted by a parton j with the larger momentum fraction $w(w > x)$ [42]. They are calculable in pQCD as a power series of α_s:

$$P_{ij}(w,\alpha_s) = \frac{\alpha_s}{2\pi}P^0_{ij}(w) + \Big(\frac{\alpha_s}{2\pi}\Big)^2 P^1_{ij}(w) + ... \tag{1.35}$$

The DGLAP equation is formally derived in the leading logarithmic approximation (LLA), where the terms of $(\alpha_s ln(Q^2))^n$ are summed up to all orders. These $(\alpha_s ln(Q^2))^n$ terms correspond to the ladder diagrams with n gluons emission as shown in figure 1.2. The LLA approximation is that the emissions are strongly ordered by transverse momentum of gluons k_T as

$$Q^2 \gg k^2_{T_n} \gg .... \gg k^2_{T_2} \gg k^2_{T_1}. \tag{1.36}$$

The approximation is valid at large enough Q^2 where α_s is small and all the contributing

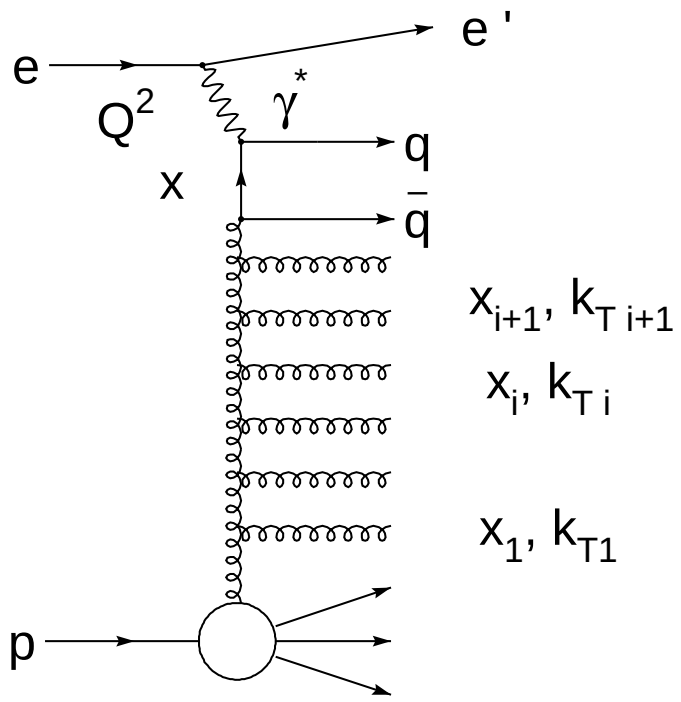

Figure 1.2: Ladder diagram for DIS in LLQ^2

terms proportional to $\alpha_s ln(\frac{1}{x})$ can be neglected.

A special case for which the DGLAP equations can be solved analytically occurs when in addition to the above conditions also strong ordering in x is required,

$$x_n \ll x_{n-1} \ll ..... \ll x_1 \ll x_0. \tag{1.37}$$

The large logarithmic terms arising from the integration are then of the form proportional to $(\alpha_s(Q^2)ln(Q^2/Q_0^2)ln(1/x))^n$, which need to be resumed. This is the double leading log approximation (DLL).

In general the structure function can be evaluated by solving the evolution equations like Dokshitzer-Gribov-Lipatov-Altarelli-Parisi (DGLAP) equation, Balitskij-Kuraev-Fadin-Lipatov (BKFL) equation [43,44] , Ciafaloni-Catani-Fiorani-Marchesini (CCFM) equation [45, 46], Gribov-Levin-Ryskin (GLR) equation [47], Modified DGLAP (MD-DGLAP) equation [48–50], Jalilian-Marian-Iancu-McLerran-Weigert-Leonidov-Kovner (JIMWLK) equation [51, 52], Balitsky-Kovchegov (BK) equation, [53, 54] etc. Among these the DGLAP evolution equation is the most familiar re-summation approach. Once a quark structure function at some reference point is given, one can compute it for any value of Q^2 using this equation. In the framework of the DGLAP equation the parton distributions grows at small-x as a result of their Q^2-evolution [41, 55].

1.5 Longitudinal Structure Function

The proton longitudinal structure function F_L, measured in DIS experiment, is one of the important observables to study. The measurement of F_L structure function is of great theoretical importance since it may allow us to distinguish between the behaviour of the different partonic distributions in the nucleon at small-x. F_L structure function is a very sensitive QCD characteristic as it is directly sensitive to the gluon density in the proton [56]. In the naive QPM, helicity is not conserved at the hadronic vertex during the interaction between the longitudinally polarised virtual photon and a quark, as illustrated in figure 1.3(a). So, the longitudinally polarized virtual photons do not couple to the spin-$\frac{1}{2}$ quarks with negligible transverse momentum and this leads to $F_L = 0$ [56]. On the other hand, in QCD improved parton model, quarks interact through gluons, and also can radiate gluons, figure 1.3(b). The gluon radiation results

in a transverse momentum component of the quark and now helicity is conserved at the hadronic vertex. As a result, quark can couple to longitudinally polarised virtual photon and the Callan-Gross relation is no longer satisfied exactly. Thus in QCD, the F_L structure function is non-zero.

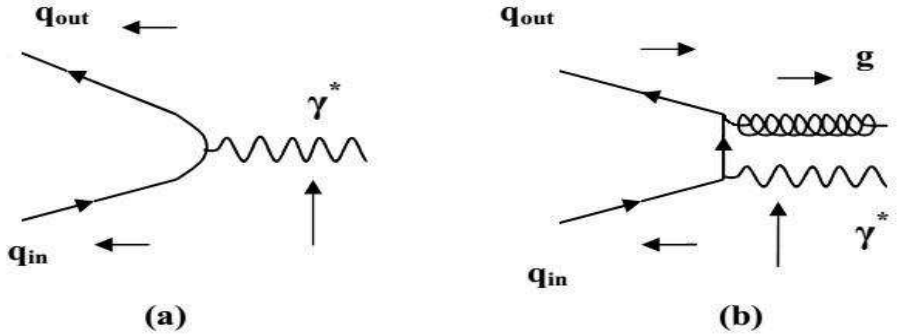

Figure 1.3: Helicity conservation at hadronic vertex in QPM (a) and QCD improved parton model (b). The arrows represent the spin orientations [57].

The one-loop virtual correction to $\gamma q \to q$ process does not contribute to the longitudinal part of the hadronic tensor $W^L_{\gamma q}$ [58] and to the order α_s the calculation of longitudinal part of this tensor gives

$$W^L_{\gamma q} = \frac{1}{3}\frac{\alpha_s}{2\pi} e_q^2 \frac{Q^2}{w} + O(\epsilon) \tag{1.38}$$

and

$$W^L_{\gamma g} = \frac{1}{2}\frac{\alpha_s}{2\pi} e_q^2 \frac{Q^2(1-w)}{w} + O(\epsilon) \tag{1.39}$$

for the contributing processes $\gamma q \to qg$ and $\gamma g \to q\bar{q}$ respectively. The contributions of ϵ-order are defined by the factorization scheme. Thus the structure functions of the gluon emission processes are expressed by the relations [59]

$$F_1^{\gamma q}(x, Q^2) = \frac{1}{2x} F_2^{\gamma q}(x, Q^2) - \sum_{q,\bar{q}} e_q^2 \frac{\alpha_s}{2\pi} \int_x^1 \frac{dw}{w} \frac{4}{3} \frac{x}{w} q(w, Q^2) \tag{1.40}$$

and

$$F_1^{\gamma g}(x,Q^2) = \frac{1}{2x}F_2^{\gamma q}(x,Q^2) - \sum_{q,\bar{q}} e_q^2 \frac{1}{2}\frac{\alpha_s}{2\pi}\int_x^1 \frac{dw}{w} g(w,Q^2) 4\frac{x}{w}\Big(1-\frac{x}{w}\Big). \tag{1.41}$$

Combining the above results, the expression for F_L structure function at LO can be written as

$$\begin{aligned} F_L(x,Q^2) &= F_2(x,Q^2) - 2xF_1(x,Q^2) \\ &= \frac{\alpha_s}{4\pi}\int_x^1 \frac{dw}{w}\Bigg[\frac{16}{3}\Big(\frac{x}{w}\Big)^2 \sum_{q,\bar{q}} e_q^2 wq(w,Q^2) \\ &\quad +8\sum_{q,\bar{q}} e_q^2\Big(\frac{x}{w}\Big)^2\Big(1-\frac{x}{w}\Big) wg(w,Q^2)\Bigg]. \end{aligned} \tag{1.42}$$

The equation (1.41) in terms of F_2 structure function and gluon distribution function can be expressed as

$$\begin{aligned} F_L(x,Q^2) &= \frac{\alpha_s}{4\pi}\int_x^1 \frac{dw}{w}\Bigg[\frac{16}{3}\Big(\frac{x}{w}\Big)^2 \sum_{q,\bar{q}} e_q^2 F_2(w,Q^2) \\ &\quad +8\sum_{q,\bar{q}} e_q^2\Big(\frac{x}{w}\Big)^2\Big(1-\frac{x}{w}\Big) wg(w,Q^2)\Bigg]. \end{aligned} \tag{1.43}$$

This equation (1.42) is known as Altarelli-Martinelli equation [18, 59]. Here the first term in the integral corresponds to the gluon radiation off a quark and the second term represents the gluon splitting into a quark anti-quark pair. Again the above equation for F_L structure function in terms of co-efficient function is given by [59, 60]

$$x^{-1}F_L = C_{L,ns} \otimes q_{ns} + < e^2 > (C_{L,s} \otimes q_s + C_{L,g} \otimes g). \tag{1.44}$$

Here q_{ns}, q_s and g are the flavour non-singlet, flavour singlet and gluon distribution function, $< e^2 >= \frac{5}{18}$ is the average squared charge for N_f (number of active light flavours) and the symbol $\otimes$ represents the standard Mellin convolution. $C_{L,a}(a = q, g)$'s

are the co-efficient functions which can be written by the perturbative expansion as follows [60]

$$C_{L,a}(\alpha_s, x) = \sum_{n=1} \left(\frac{\alpha_s}{4\pi}\right)^n C^n_{L,a}(x). \tag{1.45}$$

At small values of x, the gluon contribution to F_L dominates over the quark contribution [61] and F_L is driven mainly by gluons through the transition $g \to q\bar{q}$. Therefore, the measurement of F_L structure function can give the gluon distribution inside the proton. It also provides an important cross check of the standard picture of low-x dynamics [62].

1.6 Heavy Quarks in Proton

The heavy quarks in the proton play an pivotal role in particle physics and their production in *ep* collision provides an exciting testing ground for pQCD. The measurement of the charm and beauty quark production cross section in DIS is important for understanding the parton densities in the nucleon. The top quark is the heaviest one among the heavy quarks and due to its heavy mass it quickly decays without forming hadron. The creation of top quark pair is not possible within the range of centre of mass energy at HERA.

In the neutral current DIS process, the production of heavy quarks is mainly described by two mechanisms:

- According to the first mechanism, named as intrinsic heavy quark production, one assumes that, along with the light quarks u, d and s and the gluon g, the wave function of the proton also consists of the heavy quarks c, b, t [25, 63]. Within the context of QCD improved parton model the virtual photon interacts with the heavy quark which emerges directly from the proton.

- In the case of second mechanism known as extrinsic heavy quark production the

proton wave function does not contain the heavy quark components. In the lowest order perturbation theory the heavy quark and heavy anti-quark appear in pairs and are produced via BGF process as shown in figure 1.4.

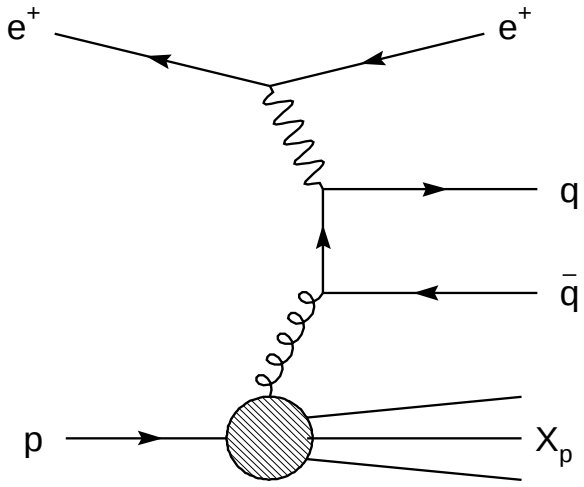

Figure 1.4: Leading order Boson Gluon Fusion (BGF) diagram for heavy quark production in ep-collisions.

In this process the quarks can be heavy if the center of mass energy squared of the $\gamma g \to q\bar{q}$ interaction is :

$$(\gamma + g)^2 > 2m_q^2, \tag{1.46}$$

where m_q^2 is the mass of the heavy quark and the photon and gluon four momentum are respectively γ and g.

The charm quark anti-quark ($c\bar{c}$) pair can be produced above the charm threshold, $Q^2 \approx (2m_c)^2$ and above the beauty threshold, the $b\bar{b}$ pair can be created. Charm contributes to the cross section mainly at small-x and higher Q^2, where the sea quark dominates the cross section. Among the charm and beauty contribution to the cross section, beauty quark contributes less to the cross section due to the coupling to its electric charge, $e_b = -\frac{1}{3}$ [57].

The dominant process for the charm and beauty quark production at HERA is the BGF shown in figure 1.4, where the photon interacts with a gluon from the proton by

the exchange of a heavy quark pair [16, 64]. Due to the presence of gluon in the initial state, this process is directly sensitive to the gluon density inside the proton. This type of process is the dominant one in DIS scattering and is particularly important at small values of x and large Q^2, due to the large gluon density [64].

The differential cross section for the charm and beauty production which directly follows from equation 1.18 can be written as

$$\frac{d^2\sigma^h}{dxdQ^2} = \frac{2\pi\alpha^2 Y_+}{xQ^4}\Big[F_2^h(x,Q^2) - \frac{y^2}{Y_+}F_L^h(x,Q^2)\Big] \tag{1.47}$$

where $h = c, b$. Both the quantities F_2^h and F_L^h are dominated by the gluon content in the proton. In the standard factorization approach to pQCD the structure functions F_k can be written as [65, 67]

$$F_k^h(x,Q^2,m_h^2) = e_h^2\frac{\alpha_s(\mu^2)}{\pi}\int_{ax}^1 \frac{dw}{w}C_{k,g}^h(w,\zeta)G\Big(\frac{x}{w},\mu^2\Big), \tag{1.48}$$

where $k = 2, L$, $a = 1 + 4\zeta(\zeta = \frac{m_h^2}{Q^2})$ and the renormalization scale μ is assumed to be either $\mu^2 = 4m_h^2$ or $\mu^2 = 4m_h^2 + Q^2$. $C_{k,g}^h$ is the heavy quark co-efficient function represented in $\overline{MS}$ scheme [67]. The heavy quark co-efficient functions differ significantly from those of the light quarks. So, the scaling violations of heavy flavour part in $F_{2,L}(x,Q^2)$ are different from those of the light flavour contribution [64]. Both for the measurement of the QCD scale Λ_{QCD} and for the extraction of the light parton densities a correct description of the heavy flavour contribution is required.

The charm and beauty production cross section has been measured in DIS using different techniques like D or D^* meson analysis [68–70], the long lifetime of heavy flavoured hadrons [71–73] or their semi leptonic decays [74].

1.7 Small-x Physics

The study of the small-x region in DIS is important for understanding the structure of the proton. The region of small-x below 0.001 is mainly dominated by the gluon

distribution in the proton [61]. In this region, the gluons in the proton form a strongly correlated system of interacting particle. The gluon densities grow rapidly as $x \to 0$ for all values of Q^2. Such types of small-x behaviour of gluon distribution function was extracted at HERA, which is shown in figure 1.5.

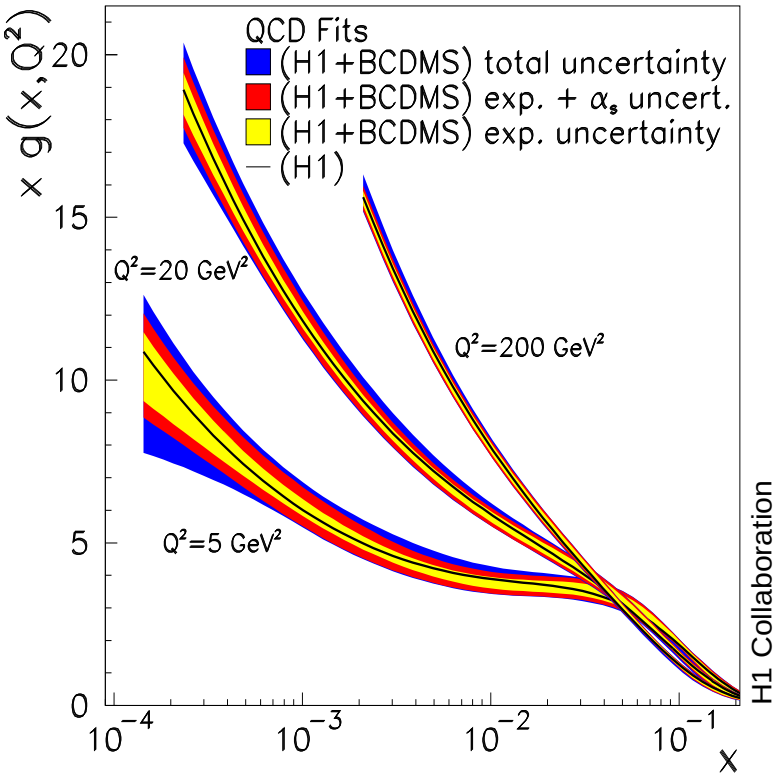

Figure 1.5: Gluon distribution function extracted at HERA [11].

This strong rise leads to a rise of the proton structure function F_2 and F_L. Such types of behaviour is well described in the framework of DGLAP evolution equations [35, 39, 41]. However, at very small values of x, when the density of gluons becomes large enough they starts overlapping in the phase space. In this case the recombination and annihilation of gluons becomes important, otherwise this strong rise leads to the violation of unitarity [75]. This effect is known as parton saturation. Such types of phenomena are explained by non-linear evolution equations.

The small-x region of the DIS offers a unique possibility to investigate the Regge

limit of pQCD [76–79]. DIS corresponds to the region where both ν and Q^2 are large. The small-x limit of DIS corresponds to case when $2M\nu >> Q^2$ which is equivalent to $s >> Q^2$ i.e., to the limit when the center of mass energy squared, s, is large and much greater than Q^2. The limit of large ν and $2M\nu >> Q^2$ is therefore the Regge limit of DIS [76]. Regge trajectory represents the exchange of a family of resonances having distinct spins. It can be asserted with confidence that the Regge theory is one of the most successful approaches for the description of high-energy scattering of hadrons. This high-energy behavior can be described by two contributions: an effective Pomeron with its intercept $\alpha_P \simeq 1.08$ slightly above unity and the leading meson Regge trajectories with the intercept $\alpha_R(0) \approx 0.5$ [80]. In Regge theory the structure function (cross section) is expected to increase approximately like a power of x towards small-x. However, at small-x the behaviour of the structure function is mainly driven by the gluons. Therefore, the behaviour of the power law rise of gluon distribution function at small-x observed at HERA is given by [81] $G(x, Q^2) \propto x^{-\lambda_g}$, where λ_g is the gluon distribution function exponent.

HERA collider made it possible to experimentally explore the small-x region. The high-energy or small-x region of DIS experiment at HERA provides a good opportunity to study the high-energy limit of QCD. One of the first observations at HERA was the strong rise of structure function F_2 towards small-x which reflects the rise of gluon density in the proton in this kinematical region [32, 82]. This was the remarkable starting point for further investigation of the structure of proton at DESY. At very small-x, saturation of the growth of the parton densities is expected, as otherwise unitarity bounds would be violated. Models based on saturation are hugely successful in describing HERA data, particularly in the low x and low Q^2 region where DGLAP approach fails.

1.8 Measurement of F_L Structure Function

Measurement of F_L structure function is a technically challenging experimental task. This structure function has a significant contribution to the cross section at high inelasticity y [21]. The direct method to obtain the F_L is to measure the DIS cross section at fixed values of x and Q^2 and different y [11]. The values of the structure function F_L were determined according to equation (1.19) by a straight-line fits to the reduced cross section as a function of y^2/Y_+ at given values of x and Q^2 and different values of center of mass energies s [11]. From the relation $Q^2 = sxy$, it is clear that the variation in y value can be obtained by varying s, the center of mass energy. Since $s = 4E_eE_p$, this could be done by varying the electron, proton or both beam energies. But in the experiment it was decided to lower the proton beam energy because reducing the electron beam energy would have required to lower the energy of the scattered electron below the trigger threshold. This would have affected the scattered electron angle more than that reduction the proton beam energy. Another advantage of lowering the proton beam is the maximum cancellation of systematics when making a relative measurement of the cross section [83]. Figure 1.5 illustrates the measurement of F_L from σ_r by the H1 collaboration [11]. Here the reduced cross section σ_r is plotted for six values of x at $Q^2 = 6.5GeV^2$, measured for proton beam energies 920, 575 and 460 GeV. The inner error bars represents the statistical error, the outer error bars show statistical and systematic uncertainties added in quadrature. The slope of the straight-line fits is determined by the structure function $F_L(x, Q^2)$ [11].

The direct measurement of F_L in the past fixed target experiments EMC (European Muon Collaboration) [84], NMC (New Muon Collaboration) [85], BCDMS (Bologna CERN Dubna Munich Saclay) [33] and SLAC [86] have been done by measuring the cross section ratio R. These measurements are at relatively high x where the sensitivity to the gluon densities is small.

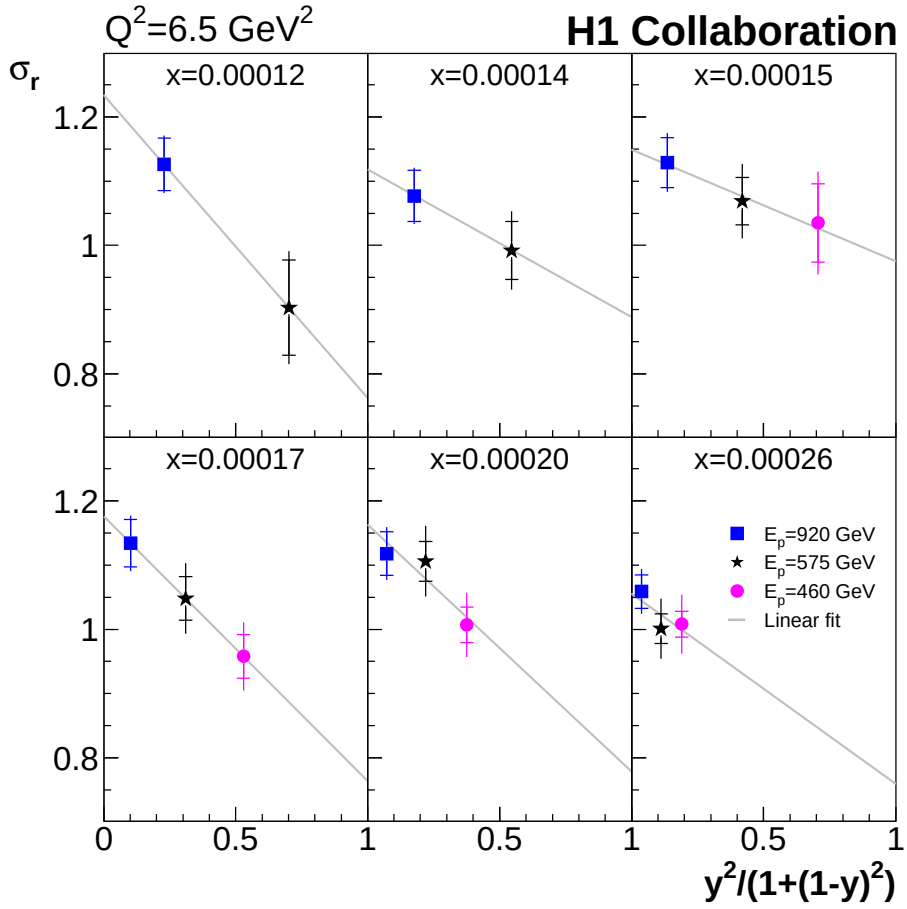

Figure 1.6: The reduced DIS cross section as a function of $y^2/(1+(1-y)^2)$ [11]

At HERA collider $F_L(x, Q^2)$ was mainly measured by H1 and ZEUS detector. An important advantage of HERA, compared to fixed target DIS lepton-nucleon experiments, is the wide range of y (inelasticity) values covered [56]. HERA collected ep collision data at a positron beam energy of 27.5 GeV and a proton beam energies of 920, 575 and 460 GeV, which allowed a measurement of structure functions at x values $2.9 \times 10^{-5} \leq x \leq 0.01$ and Q^2 values $1.5 GeV^2 \leq Q^2 \leq 800 GeV^2$ [11, 12].

1.9 Some of the DIS Experiments Related to F_L

European Muon Collaboration(EMC) : In the muon scattering experiment performed by European Muon Collaboration (EMC) at CERN (Conseil Europeen pour la Recherche Nucleaire) SPS (Super Proton Synchrotron), the structure function F_2 and R were measured with muon beams energies 120, 200, 240 and 280 GeV. Here the target materials were proton (p), deuterium (D), iron (Fe), calcium (Ca), copper (Cu), tin (Sn) and carbon (C). The kinematical range of measurement were: $0.0175 \leq x \leq 0.75$ and $2.5 \leq Q^2 \leq 170 GeV^2$ for $F_2(p)$ and $0.114 \leq x \leq 0.231$ and $15 \leq Q^2 \leq 65 GeV^2$ for $R(p)$ [84]; $0.05 \leq x \leq 0.65$ and $9 \leq Q^2 \leq 200 GeV^2$ for $F_2(Fe)$ [87]; $0.0025 \leq x \leq 0.75$ and $0.25 \leq Q^2 \leq 170 GeV^2$ for $F_2(D)$ [88, 89]; $0.0031 \leq x \leq 0.612$ and $0.52 \leq Q^2 \leq 46.4 GeV^2$ for the ratios $F_2(C)/F_2(D)$, $F_2(Cu)/F_2(D)$, $F_2(Ca)/F_2(D)$ and $F_2(Sn)/F_2(D)$ [89–92].

New Muon Collaboration (NMC) : The New Muon Collaboration (NMC) measured the structure function F_2 and R in muon scattering experiment at the CERN SPS with muon beams of energies 90, 120, 200, and 280 GeV. The target materials were p, D, helium (He), lithium (Li), C, Ca, Fe, Sn and lead (Pb). The kinematical range of measurement were: $0.001 \leq x \leq 0.6$ and $0.5 \leq Q^2 \leq 75 GeV^2$ for $F_2(p)$ and $F_2(D)$ [85, 93, 94]; $0.0045 \leq x \leq 0.11$ and $1.38 \leq Q^2 \leq 20.6 GeV^2$ for $R(p)$ [85]; $0.003 \leq x \leq 0.7$ and $0.12 \leq Q^2 \leq 100 GeV^2$ for the ratio $F_2(p)/F_2(D)$ [95–97]; $0.007 \leq x \leq 0.8$ and $0.6 \leq Q^2 \leq 18.3 GeV^2$ for the ratios $F_2(Ca)/F_2(Li)$, $F_2(C)/F_2(Li)$ and $F_2(Ca)/F_2(C)$ [98]; $0.0035 \leq x \leq 0.65$ and $0.5 \leq Q^2 \leq 90 GeV^2$ for the ratios $F_2(He)/F_2(D)$, $F_2(C)/F_2(D)$ and $F_2(Ca)/F_2(D)$ [99].

Bologna CERN Dubna Munich Saclay Collaboration (BCDMS) : The Bologna CERN Dubna Munich Saclay Collaboration measured the structure function

F_2 and R in muon scattering experiment at CERN. The incident muon beam energies are 100, 120, 200, 280 GeV and the target material used were p, D, C, Fe and nitrogen (N). The kinematical range of measurement were: $0.07 \leq x \leq 0.75$ and $7.5 \leq Q^2 \leq 230 GeV^2$ for $F_2(p)$ [33]; $0.07 \leq x \leq 0.65$ and $15 \leq Q^2 \leq 85 GeV^2$ for $R(p)$, $R(D)$ and $R(C)$ [33, 100, 101]; $0.07 \leq x \leq 0.75$ and $8.75 \leq Q^2 \leq 252.5 GeV^2$ for $F_2(C)$ and $F_2(D)$ [100, 101]; $0.02 \leq x \leq 0.7$ and $14 \leq Q^2 \leq 200 GeV^2$ for the ratios $F_2(Fe)/F_2(D)$ and $F_2(N)/F_2(D)$ [102, 103].

Stanford Linear Accelerator Center (SLAC) : In the deep inelastic electron scattering experiment performed at SLAC, structure function F_2 and R were measured with electron beam energies up to 50 GeV. Here the main target material used were p, D, Fe and gold (Au). The kinematical range of measurement were: $0.2 \leq x \leq 0.5$ and $1 \leq Q^2 \leq 10 GeV^2$ for $F_2(D)$, $F_2(Fe)$, $F_2(Au)$ and $R(D)$, $R(Fe)$, $R(Au)$ [23]; $0.03 \leq x \leq 0.1$ and $1.3 \leq Q^2 \leq 2.7 GeV^2$ for $R(C)$ [104].

H1 : The H1 collaboration determined the structure function F_2 and F_L from the cross section measurement in electron proton scattering experiment with the H1 detector at HERA. Here the data were taken with the lepton beam energy of 27.6 GeV and a proton beam energies of 920, 575 and 460 GeV. The measurement covers the region $10^{-6} \leq x \leq 0.1$ and $1.5 \leq Q^2 \leq 10^4 GeV^2$ for F_2 and $2.9 \times 10^{-5} \leq x \leq 0.1$ and $1.5 \leq Q^2 \leq 800 GeV^2$ for F_L up to $y = 0.85$ [11, 12, 32, 105]. Inclusive charm and beauty cross sections are also measured in $e^- p$ and $e^+ p$ neutral current collisions at HERA with the H1 detector in the kinematic region $5 \leq Q^2 \leq 2 \times 10^3 GeV^2$ and $2 \times 10^{-4} \leq x \leq 0.05$ [13, 71, 72].

ZEUS : The ZEUS collaboration determined the structure function F_2 and F_L from the cross section measurement in electron proton scattering experiment with the ZEUS detector at HERA. The data were taken with the lepton beam energy of 27.6 GeV and a proton beam energies of 920, 820, 575 and 460 GeV. The measurement

covers the region $10^{-4} \leq x \leq 0.1$ and $10 \leq Q^2 \leq 10^4 GeV^2$ for F_2 and $10^{-4} \leq x \leq 0.1$ and $5 \leq Q^2 \leq 130 GeV^2$ for F_L with y value $0.09 \leq y \leq 0.78$ [106–108]. The charm and beauty structure functions F_2^c and F_2^b were also measured with the ZEUS detector at HERA. Data covers the region $10 \leq Q^2 \leq 10^3 GeV^2$ and $10^{-4} \leq x \leq 0.1$ [73, 74, 109].

References

[1] Glashow, S. L. Partial-symmetries of weak interactions, *Nucl. Phys.* **22** (4), 579–588, 1961.

[2] Salam, A. and Ward, J. C. Electromagnetic and weak interactions, *Phys. Lett.*, **13** (2), 168-171, 1964.

[3] Gross, D. J. and Wilczek, F. Asymptotically free gauge theories, *Phys. Rev. D* **8** (10), 3633–3652, 1973.

[4] Politzer, H. D. Asymptotic freedom: an approach to strong interactions, *Phys. Rept.* **14** (4), 129–180, 1974.

[5] Gross, D. J. and Wilczek, F. Ultraviolet behavior of non-abelian gauge theories, *Phys. Rev. Lett.* **30** (26), 1343–1346, 1973.

[6] Weinberg, S. Non-abelian gauge theories of the strong interactions, *Phys. Rev. Lett.* **31** (7), 494–497, 1973.

[7] Wilson, K. G. Confinement of qnarks, *Phys. Rev. D* **10** (8), 2445–2459, 1974.

[8] Rutherford, E. The scattering of α and β particles by matter and the structure of the atom, *Philos. Mag.* **21** (125), 669–688, 1911.

[9] Bloom, E. D., et al. High-energy inelastic *ep* scattering at6-degrees and 10-degrees, *Phys. Rev. Lett.* **23** (16), 930–934, 1969.

[10] Breidenbach, M., et al. Observed behaviour of highly inelastic electron-proton scattering, *Phys. Rev. Lett.* **23** (16), 935–939, 1969.

[11] Aaron, F. D., et al. Measurement of the inclusive $e^{\pm}p$ scattering cross section at high inelasticity y and of the structure function F_L, *Eur. Phys. J. C* **71** (3), 1579-1–50, 2011.

[12] Andreev, V., et al. Measurement of Inclusive *ep* Cross Sections at High Q^2 at $\sqrt{s} = 225$ and $252GeV$ and of the Longitudinal Proton Structure Function F_L at HERA, *Eur. Phys. J. C* **74** (4), 2814-1–26, 2014.

[13] Aaron, F. D., et al. Measurement of the charm and beauty structure functions using the H1 vertex detector at HERA, *Eur. Phys. J. C.* **65** (1-2), 89–109, 2010.

[14] Toll, T. and Frixione, S. Charm and bottom photoproduction at HERA with MC@NLO, *Phys. Lett. B* **703** (4), 452–461, 2011.

[15] Campbell, J., et al. Higgs-boson production in association with a single bottom quark *Phys. Rev. D* **67** (9), 095002-1–13, 2003.

[16] Carvalho, F., et al. Charm and longitudinal structure functions within the Kharzeev-Levin-Nardi model, *Phys. Rev. C* **79** (3), 035211-1–6, 2009.

[17] Devenish, R. and Cooper-Sarkar, A. M. *Deep Inelastic Scattering*, Oxford University Press, New York, 2011.

[18] Roberts, R. G. *The structure of the proton*, Cambridge University Press, New York, 1990.

[19] Halzen, F. and Martin, A. D. *Quark and Leptons: An Introductory Course in Modern Particle Physics*, John Wiley and Sons, New York, 1984.

[20] Bjorken, J. D. and Drell, S. D. *Relativistic Quantum Fields*, McGraw-Hill Book Company, New York, 1965.

[21] Glazov, S. Measurement of DIS Cross Section at HERA, *Braz. J. Phys.* **37** (2C), 793–797, 2007.

[22] Abramowicz, H., et al. Deep inelastic cross-section measurements at large y with the ZEUS detector at HERA, *Phys. Rev. D* **90** (7), 072002-1–27, 2014.

[23] Dasu, S., et al. Measurement of kinematic and nuclear dependence of $R = \sigma_L/\sigma_T$ in deep inelastic electron scattering, *Phys. Rev. D* **49** (11), 5641–5674, 1994.

[24] Feynman, R. P. Very high-energy collisions of hadrons, *Phys. Rev. Lett.* **23** (24), 1415-1417, 1969.

[25] Bjorken, J. D. Asymptotic Sum Rules at Infinite Momentum, *Phys. Rev.* **179** (5), 1547-1553, 1969.

[26] Gell-Mann, M. A schematic model of baryons and mesons, *Phys. Lett.* **8** (3), 214–215, 1964.

[27] Zweig, G. An $SU(3)$ model for strong interaction symmetry and its breaking, CERN report 8419/TH. 412, 1964.

[28] Callan, C. and Gross, D. J. High-energy electroproduction and the constitution of the electric current, *Phys. Rev. Lett.* **22** (4), 156–159, 1969.

[29] Miller, G., et al. Inelastic Electron-Proton Scattering at Large Momentum Transfers and the Inelastic Structure Functions of the Proton, *Phys.Rev. D* **5** (3), 528-544, 1972.

[30] Bodek, A., et al. Experimental Studies of the Neutron and Proton Electromagnetic Structure Functions, *Phys.Rev. D* **20** (7), 1471-1552, 1979.

[31] Mesteyer, M. D., et al. Ratio σ_L/σ_T from deep-inelastic electron scattering, *Phys.Rev. D* **27** (1), 285-288, 1983.

[32] Abt, I., et al. Measurement of the proton structure function $F_2(x, Q^2)$ in the low-x region at HERA, *Nucl. Phys. B* **407** (3), 515–535, 1993.

[33] Benvenuti, A., et al. A High Statistics Measurement of the Proton Structure Functions $F_2(x, Q^2)$ and R from Deep Inelastic Muon Scattering at High Q^2, *Phys. Lett. B* **223** (3-4), 485–489, 1989.

[34] Hinchliffe, I. and Manohar, A. V. The QCD Coupling Constant, *Ann. Rev. Nucl. Part. Sci.* **50** (2000), 643–678, 2000.

[35] Altarelli, G. and Parisi, G. Asymptotic freedom in parton language, *Nucl. Phys. B.* **126** (2), 298–318, 1977.

[36] Collins, John C., et al. Factorization of Hard Processes in QCD, *Adv. Ser. Direct. High Energy Phys.* **5** (1988), 1-91, 1988.

[37] Collins, John C., et al. Factorization for short distance hadron-hadron scattering, *Nucl. Phys. B* **261** 104–142, 1985.

[38] Narison, S. *QCD as a theory of hadrons: From Partons to Confinement*, Cambridge University Press, New York, 2004.

[39] Gribov, V. N. and Lipatov, L. N. Deep inelastic ep scattering in perturbation theory, *Sov. J. Nucl. Phys.* **15** (4), 438–450, 1972.

[40] Lipatov, L. N. The parton model and perturbation theory, *Sov. J. Nucl. Phys.* **20** (1), 94–102, 1975.

[41] Altarelli, G. Partons in quantum chromodynamics, *Phys. Rep* **81** (1), 1–129, 1982.

[42] Cooper-Sarkar, A. M., Devenish R. C. E., and Roeck, A. D. E. Structure functions of the nucleon and their interactions, *Int. J. Mod. Phys. A* **13** (20), 3385–3586, 1998.

[43] Kuraev, E. A., Lipatov, L. N., and Fadin, V. S. The Pomeranchuk singularity in nonabelian gauge theories, *Sov. Phys. JETP* **45** (2), 199–204, 1977.

[44] Balitskii, Y. Y. and Lipatov, L. N. The Pomeranchuk Singularity in Quantum Chromodynamics, *Sov. J. Nucl. Phys.* **28** (6), 822–829, 1978.

[45] Catani, S., Fiorani, F. and Marchesini, G. QCD coherence in initial state radiation, *Phys. Lett. B* **234** (3), 339–345, 1990.

[46] Ciafaloni, M. QCD coherence in initial state radiation, *Nucl. Phys. B* **296** (1), 49–74, 1988.

[47] Gribov, L. V., Levin, E. M. and Ryskin, M. G. Semihard processes in QCD, *Phys. Rep.* **100** (1-2), 1–150, 1983.

[48] Zhu, W. A new approach to parton recombination in the QCD evolution equations, *Nucl. Phys. B* **551** (1-2), 245–274, 1999.

[49] Zhu, W. and Ruan, J. H. A new modified Altarelli-Parisi evolution equation with parton recombination in proton, *Nucl. Phys. B* **559** (1-2), 378–392, 1999.

[50] Zhu, W., Shen, Z. Q. and Ruan, J. H. Parton recombination effect in polarized parton distributions, *Nucl. Phys. B* **692** (3) 417–433, 2004.

[51] Jalilian Marian, J., et al. The BFKL equation from the Wilson renormalization group, *Nucl. Phys. B* **504** (1-2), 415–431, 1997.

[52] Iancu, E., Leonidov, A. and McLerran, L. Nonlinear gluon evolution in the color glass condensate: I, *Nucl. Phys. A* **692** (3-4), 583–645, 2001.

[53] Balitsky, I. Operator expansion for high-energy scattering, *Nucl. Phys. B* **463** (1), 99–157, 1996.

[54] Kovchegov, Yu. Small-x F_2 structure function of a nucleus including multiple Pomeron exchanges, *Phys. Rev. D* **60** (3), 034008,1–8, 1999.

[55] Lipatov, L. N. Small-x physics in perturbative QCD, *Phys. Rept.* **286**, (3), 131–198, 1997.

[56] Gogitidze, N. Determination of the longitudinal structure function F_L at HERA, *J. Phys. G: Nucl. Part. Phys.* **28** (5), 751–765, 2002.

[57] Tuning, N. *Proton structure functions at HERA*, PhD thesis, University of Amsterdam, Netherland, 2001.

[58] Dissertori, G., Knowles, I.G. and Schmelling, M. *Quantum Chromodynamics: High Energy Experiments and Theory*, Oxford University Press, North Carolina, U.S.A, 2003.

[59] Altarelli, G. and Martinelli, G. Transverse momentum of jets in electroproduction fromquantum chromodynamics, *Phys. Lett. B* **76** (1), 89–94, 1978.

[60] Moch, S., Vermaseren, J. A. M. and Vogt, A. The longitudinal structure function at the third order, *Phys. Lett. B* **606** (1-2), 123–129, 2005.

[61] Cooper-Sarkar, A. M., et al. Measurement of the longitudinal structure function and the small x gluon density of the proton, *Z. Phys. C* **39** (2), 281–290, 1988.

[62] Galzov, A. Recent measurements of the proton structure functions at HERA, *Acta Phys. Pol. B Proc. Suppl.* **1** (2), 371–378, 2008.

[63] Feynmann, R. P. Very high-energy collisions of hadrons, *Phys. Rev. Lett.* **23** (24), 1415–1417, 1969.

[64] Behnke, O. Open Charm and Beauty Production at HERA, *Nucl. Phys. B (Proc. Suppl.)* **222-224** 140-150, 2012.

[65] Gluck, M., Reya, E. and Vogt, A. Dynamical parton distributions of the proton and small x physics, *Z. Phys. C* **67** (3), 433–447, 1995.

[66] Gluck, M., Reya, E. and Vogt, A. Dynamical parton distributions revisited, *Eur. Phys. J. C* **5** (3), 461–470, 1998.

[67] Catani, S., Ciafaloni, M. and Hautmann, F. High energy factorization and small-x heavy flavour production, *Nucl. Phys. B* **366** (1), 135–188, 1991.

[68] Breitweg, J., et al. Measurement of $D^{*\pm}$ production and the charm contribution to F_2 in deep inelastic scattering at HERA, *Eur. Phys. J. C* **12** (1), 35–52, 2000.

[69] Adloff, C., et al. Measurement of $D^{*\pm}$ meson production and F_2^c in deep-inelastic scattering at HERA, *Phys. Lett. B* **528**, (3-4), 199–214, 2002.

[70] Abramowicz, H., et al. Measurement of D^+ and Λ_c^+ production in deep inelastic scattering at HERA, *J. High Energy Phys.* **2010** (11), 009-1-27, 2010.

[71] Aktas, A., et al. Measurement of $F_2^{c\bar{c}}$ and $F_2^{b\bar{b}}$ at high Q^2 using the H1 vertex detector at HERA, *Eur. Phys. J. C* **40** (3), 349–359, 2005.

[72] Aktas, A., et al. Measurement of $F_2^{c\bar{c}}$ and $F_2^{b\bar{b}}$ at low Q^2 and x using the H1 vertex detector at HERA, *Eur. Phys. J. C* **45**, (1), 23–33, 2006.

[73] Chekanov, S., et al. Measurement of $D^{\pm}$ and D^0 production in deep inelastic scattering using a lifetime tag at HERA, *Eur. Phys. J. C* **63** (2), 171–188, 2009.

[74] Chekanov, S., et al. Measurement of charm and beauty production in deep inelastic ep scattering from decays into muons at HERA, *Eur. Phys. J. C* **65** (1-2), 65–79, 2010.

[75] Mueller, A. H. and Qiu, J. Gluon recombination and shadowing at small values of x, *Nucl. Phys. B* **268** (2), 427–452, 1986.

[76] Collins, P. D. B. *Introduction to regge theory and high energy physics*, Cambridge University Press, New York, 1977.

[77] Soyez, G. Small-Q^2 extension of DGLAP-constrained Regge residues, *Phys. Lett. B* **603** (3-4), 189–194, 2004.

[78] Drescher, H. J., et al. Parton based Gribov Regge theory, *Phys. Rep.* **350** (2-4), 93–289, 2001.

[79] Desgrolard, P. and Martynov, E. Regge models of the proton structure function with and without hard pomeron: A comparative analysis, *Eur. Phys. J. C* **22** (3), 479–492, 2001.

[80] Donnachie, A. and Landshoff, P. V. Perturbative QCD and Regge theory: closing the circle, *Phys. Lett. B* **533** (3-4), 277–284, 1992.

[81] Kotikov, A. V. and Parente, G. The gluon distribution as a function of F_2 and $dF_2/dlnQ^2$ at small x. The next-to-leading analysis, *Phys. Lett. B* **379** (1-4), 195–201, 1996.

[82] Derrick, M., et al. Measurement of the Proton Structure Function F_2 in ep Scattering at HERA, *Phys. Lett. B* **316** (2-3), 412–426, 1993.

[83] Adloff, C. Measurement of inclusive jet cross sections in photoproduction at HERA, *Eur. Phys. J. C* **29** (4), 497–513, 2003.

[84] Aubert, J. J., et al. A detailed study of the proton structure functions in deep inelastic muon-proton scattering, *Nucl. Phys. B* **259** (2-3), 189–265, 1985.

[85] Arneodo, M., et al. Measurement of the proton and deuteron structure functions, F_2^p and F_2^d, and of the ratio σ_L/σ_T, *Nucl. Phys. B* **483** (1-2), 3-43, 1997.

[86] Whitlow, L. W., et al. A precise extraction of $R = \sigma_L/\sigma_T$ from a global analysis of the SLAC deep inelastic $e - p$ and $e - d$ scattering cross sections, *Phys. Lett. B* **250** (1-2), 193–198, 1990.

[87] Aubert, J. J., et al. A detailed study of the nucleon structure functions in deep inelastic muon scattering in iron, *Nucl. Phys. B* **272** (1), 158–192, 1986.

[88] Aubert, J. J., et al. Measurements of the nucleon structure functions F_2^N in deep inelastic muon scattering from deuterium and comparison with those from hydrogen and iron, *Nucl. Phys. B* **293**, 740–786, 1987.

[89] Arneodo, M., et al. Measurements of the nucleon structure function in the range $0.002 < x < 0.17$ and $0.2 < Q^2 < 8GeV^2$ in deuterium, carbon and calcium, *Nucl. Phys. B* **333** (1), 1–47, 1990.

[90] Ashman, J., et al. Measurement of the ratios of deep inelastic muon-nucleus cross sections on various nuclei compared to deuterium, *Phys. Lett. B* **202** (4), 603–610, 1988.

[91] Arneodo, M., et al. Shadowing in deep inelastic muon scattering from nuclear targets, *Phys. Lett. B* **211** (4), 493–499, 1988.

[92] Ashman, J., et al. A Measurement of the ratio of the nucleon structure function in copper and deuterium, *Z. Phys. C* **57** (2), 211–218, 1993.

[93] Arneodo, M., et al. Accurate measurement of F_2^d/F_2^p and $R^d - R^p$, *Nucl. Phys. B* **487** (1-2), 3–26, 1997.

[94] Arneodo, M., et al. Measurement of the proton and the deuteron structure functions, F_2^p and F_2^d, *Phys. Lett. B* **364** (2), 107–115, 1995.

[95] Allasia, D., et al. Measurement of the neutron and the proton F2 structure function ratio, *Phys. Lett. B* **249** (2), 366–372, 1990.

[96] Amaudruz, P., et al. Gottfried sum from the ratio F_2^n/F_2^p, *Phys. Rev. Lett.* **66** (21), 2712–2715, 1991.

[97] Armadruz, P., et al. The ratio F_2^n/F_2^p in deep inelastic muon scattering, *Nucl. Phys. B* **371** (1-2), 3–31, 1992.

[98] Amaudruz, P., et al. Precision measurement of structure function ratios for $Li-6$, $C-12$ and $Ca-40$, *Z. Phys. C* **53** (1), 73–77, 1992.

[99] Amaudruz, P., et al. Precision measurement of the structure function ratios $F_2(He)/F_2(D)$, $F_2(C)/F_2(D)$ and $F_2(Ca)/F_2(D)$, *Z. Phys. C* **51** (3), 387–394, 1991.

[100] Benvenuti, A. C., et al. A high statistics measurement of the nucleon structure function $F_2(x, Q^2)$ from deep inelastic muon-carbon scattering at high Q^2, *Phys. Lett. B* **195** (1), 91–96, 1987.

[101] Benvenuti, A. C., et al. A high statistics measurement of the deuteron structure functions $F_2(x, Q^2)$ and R from deep inelastic muon scattering at high Q^2, *Phys. Lett. B* **237** (3-4), 592–598, 1990.

[102] Benvenuti, A. C., et al. Nuclear effects in deep inelastic muon scattering on deuterium and iron targets, *Phys. Lett. B* **189** (4), 483–487, 1987.

[103] Bari, G., et al. A measurement of nuclear effects in deep inelastic muon scattering on deuterium, nitrogen and iron targets, *Phys. Lett. B* **163** (1-4), 282–286, 1985.

[104] Abe, K., et al. Measurements of $R = \sigma_L / \sigma_T$ for $0.03 < x < 0.1$ and fit to world data, *Phys. Lett. B* **452** (1-2), 194–200, 1999.

[105] Adloff, C., et al. Measurement of neutral and charged current cross-sections in positron proton collisions at large momentum transfer, *Eur. Phys. J. C* **13** (4), 609–639, 2000.

[106] Breitweg, J., et al. Measurement of the proton structure function F_2 at very low Q^2 at HERA, *Phys. Lett. B* **487** (1-2), 53–73, 2000.

[107] Chekanov, S., et al. Measurement of the neutral current cross-section and F_2 structure function for deep inelastic e^+p scattering at HERA, *Eur. Phys. J. C* **21** (3), 443–471, 2001.

[108] Chekanov, S., et al. Measurement of the longitudinal proton structure function at HERA, *Phys. Lett. B* **682** (1), 8–22, 2009.

[109] Chekanov, S., et al. Measurement of D mesons production in deep inelastic scattering at HERA, *J. High Energy Phys.* **2007** (07) 074-1–37, 2007. □